Cell Death and Differentiation (2013) 20, 396–407

www.nature.com/cdd

Type-3 metabotropic glutamate receptors regulate chemoresistance in glioma stem cells, and their levels are inversely related to survival in patients with malignant gliomas

C Ciceroni[1], M Bonelli[2], E Mastrantoni[2], C Niccolini[2], M Laurenza[2], LM Larocca[3], R Pallini[4], A Traficante[5], P Spinsanti[2], L Ricci-Vitiani[6], A Arcella[5], R De Maria[6], F Nicoletti[2,5], G Battaglia[5,7] and D Melchiorri[*,1,2,7]

Drug treatment of malignant gliomas is limited by the intrinsic resistance of glioma stem cells (GSCs) to chemotherapy. GSCs isolated from human glioblastoma multiforme (GBM) expressed metabotropic glutamate receptors (mGlu3 receptors). The DNA-alkylating agent, temozolomide, killed GSCs only if mGlu3 receptors were knocked down or pharmacologically inhibited. In contrast, mGlu3 receptor blockade did not affect the action of paclitaxel, etoposide, *cis*-platinum, and irinotecan. mGlu3 receptor blockade enabled temozolomide toxicity by inhibiting a phosphatidylinositol-3-kinase/nuclear factor-κB pathway that supports the expression of O^6-methylguanine-DNA methyltransferase (MGMT), an enzyme that confers resistance against DNA-alkylating agents. In mice implanted with GSCs into the brain, temozolomide combined with mGlu3 receptor blockade substantially reduced tumor growth. Finally, 87 patients with GBM undergoing surgery followed by adjuvant chemotherapy with temozolomide survived for longer time if tumor cells expressed low levels of mGlu3 receptors. In addition, the methylation state of the MGMT gene promoter in tumor extracts influenced survival only in those patients with low expression of mGlu3 receptors in the tumor. These data encourage the use of mGlu3 receptor antagonists as add-on drugs in the treatment of GBM, and suggest that the transcript of mGlu3 receptors should be measured in tumor specimens for a correct prediction of patients' survival in response to temozolomide treatment.
Cell Death and Differentiation (2013) **20**, 396–407; doi:10.1038/cdd.2012.150; published online 23 November 2012

Malignant gliomas are highly infiltrating brain tumors that represent the third cause of cancer-related deaths among middle-aged men and the fourth cause of death among women between 15 and 34 years of age. The life expectancy of patients with grade IV astrocytoma (glioblastoma multiforme (GBM)) is 12 to 15 months, despite aggressive surgery, radiation, and chemotherapy.[1,2] According to the cancer stem cell hypothesis, malignant gliomas arise from mutated, developmentally arrested multipotent progenitor cells ('glioma stem cells' or GSCs), which undergo self-renewal for an unlimited period of time and sustain tumor growth.[3–6] GSCs are found in low percentage within the tumor mass,[7] but are intrinsically resistant to radiotherapy and chemotherapy because they cycle slowly and express high levels of proteins mediating mechanisms of drug resistance.[6,8] This highlights the importance of designing new classes of agents that specifically target GSCs. Multiple intracellular signaling pathways regulate proliferation, differentiation, survival, and chemoresistance of GSCs,[9] which limits the value of small-molecule inhibitors of individual pathways in the treatment of malignant gliomas.[10,11] This encourages the search for novel therapeutic targets that lie upstream of signal propagation and have a strong impact on the fate of GSCs. We found that type-3 metabotropic glutamate receptors (mGlu3 receptors), which are coupled to G_i/G_o proteins, regulate GSCs and activate multiple signal-transduction pathways in GSCs and other cell types.[12,13] Pharmacological blockade of mGlu3 receptors promotes astroglial differentiation of GSCs by facilitating the activity of bone morphogenetic proteins.[12] In mice implanted with GSCs into the brain, a 3-month systemic treatment with a potent mGlu3 receptor antagonist started at the time of cell implantation substantially reduced tumor growth.[12] These

[1]IRCCS San Raffaele Pisana, Rome 00163, Italy; [2]Department of Physiology and Pharmacology, University 'Sapienza', Rome 00185, Italy; [3]Institutes of Pathology Università Cattolica del Sacro Cuore, Rome 00186, Italy; [4]Institutes of Neurosurgery, Università Cattolica del Sacro Cuore, Rome 00186, Italy; [5]IRCCS Neuromed, Pozzilli 86077, Italy and [6]Department of Hematology, Istituto Superiore di Sanità, Rome 00161, Italy
*Corresponding author: D Melchiorri, Department of Physiology and Pharmacology, University 'Sapienza', Piazzale A Moro, 5, Rome 00185, Italy. Tel: +39 0649912969; Fax: +39 064450307; E-mail: danimelchiorri@hotmail.com
[7]The last two authors contributed equally to this work.
Keywords: metabotropic glutamate receptor mGlu3; glioblastoma; temozolomide; cancer stem cells; MGMT
Abbreviations: GSC, glioma stem cell; GBM, glioblastoma multiforme; MGMT, O^6-methylguanine-DNA methyltransferase; mGlu, metabotropic glutamate; MAP, mitogen-activated protein; PtdIns-3-K, phosphatidylinositol-3-kinase; cAMP, cyclic adenosine monophosphate; ERK, extracellular signal-regulated kinase; EGF, epidermal growth factor; EGFR, epidermal growth factor receptor; mTOR, mammalian target of rapamycin; RT-PCR, reverse transcriptase-polymerase chain reaction; OS, overall survival; DMEM, Dulbecco's modified Eagle's medium; bFGF, basic fibroblast growth factor; Sox-2, sex-determining Y-box 2; DAPI, 4,6-diamidino-2-phenylindole; GSK3, glycogen synthase kinase-3; SDS-PAGE, sodium dodecyl sulfate-polyacrylamide gel electrophoresis; MTT, 3-(4,5-dimethylthioazol-2-yl)-2,5-diphenyl tetrazolium bromide; LDH, lactate dehydrogenase; ChIP, chromatin immunoprecipitation; GFP, green fluorescent protein
Received 8.3.12; revised 8.8.12; accepted 1.10.12; Edited by S Kaufmann; published online 23.11.12

data are interesting, but they have limited value in translational medicine because the treatment of malignant gliomas in humans usually starts when the tumor is already fully developed. In pilot studies, we could not see any significant effect of the mGlu3 receptor antagonist when treatment started weeks after GSC implantation. We decided to examine whether mGlu3 receptor blockade could facilitate the cytotoxic action of conventional chemotherapeutic agents becoming effective as add-on drugs in the treatment of malignant gliomas. We report here that mGlu3 receptor blockade enables the cytotoxic action of the DNA-alkylating agent, temozolomide, on GSCs, and the combination of the two drugs is effective in reducing tumor growth in mice implanted with GCSs. In addition, we show that the expression level of mGlu3 receptors in tumor samples is inversely related to overall survival (OS) in patients with GBM undergoing surgery followed by radiotherapy and temozolomide treatment.

Results

mGlu3 receptors restrain temozolomide toxicity in cultured human GCSs. We used five clones of GSCs (named A–E) isolated from surgical specimens of human GBM. Cultured GCSs grown under proliferating conditions formed floating 'tumor spheres', in which >75–80% of cells expressed the stem cell markers, nestin, Musashi homolog 1 (Musashi1), and sex-determining Y-box 2 (Sox-2) (immunostaining of cells from clone 'E' are shown in Figure 1a; see also Hadjipanayis and Van Mier[9]). A smaller percentage of cells (22–29% of cells from clones B to E, and 40% of cells from clone A) were labeled by the AC133 antibody recognizing a glycosylated epitope of CD133.[4] Tumorigenicity of cells of clone E was confirmed by an *in vivo* dilution assay (Figure 1b).

Undifferentiated GSCs from all five clones expressed mGlu3, but not mGlu2, receptors (Figures 2a and b). mGlu3 receptors are coupled to G_i proteins, and their activation inhibits adenylyl cyclase activity, and stimulates the mitogen-activated protein kinase (MAPK) and phosphatidylinositol-3-kinase (PtdIns-3-K) pathways.[13] GCSs dissociated from the tumor spheres were starved from mitogens, and then challenged with the selective mGlu2/3 receptor agonist, (–)-2-oxa-4-aminobicyclo[3.1.0]exhane-4,6-dicarboxylic acid (LY379268). This treatment inhibited forskolin-stimulated cyclic adenosine monophosphate (cAMP) formation and increased levels of phosphorylated extracellular signal-regulated kinase (ERK)1/2 and phosphorylated Akt. All these effects were reversed by the mGlu2/3 receptor antagonist, (2*S*,1′*S*,2′*S*)-2-(9-xanthylmethyl)-2-(2′-carboxycyclopropyl)-glycine (LY341495) (Figures 2c–e reports data obtained in clone 'E'; see Supplementary Figure 1 for data in other

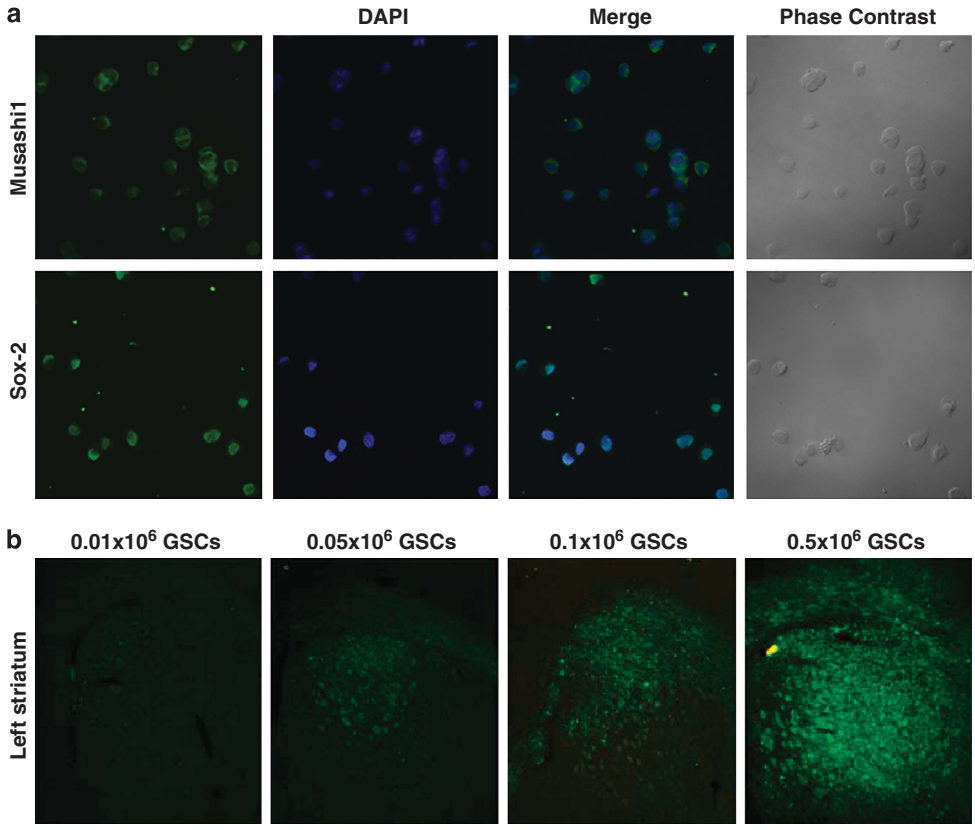

Figure 1 Expression of stem cell markers and tumorigenicity of GSCs isolated from clone E. Immunocytochemical analysis of Musashi1 and Sox-2 is shown in (**a**). Fluorescence staining is in green; DAPI, used as a counterstaining, is blue; phase-contrast microscopy is also shown. *In vivo* limiting dilution assay of GSCs implanted in the striatum of mice killed 3 months later is shown in (**b**). Representative images show the presence of 0.01, 0.05, 0.1, and 0.5×10^6 GFP^+ GSCs in the striatum of implanted mice

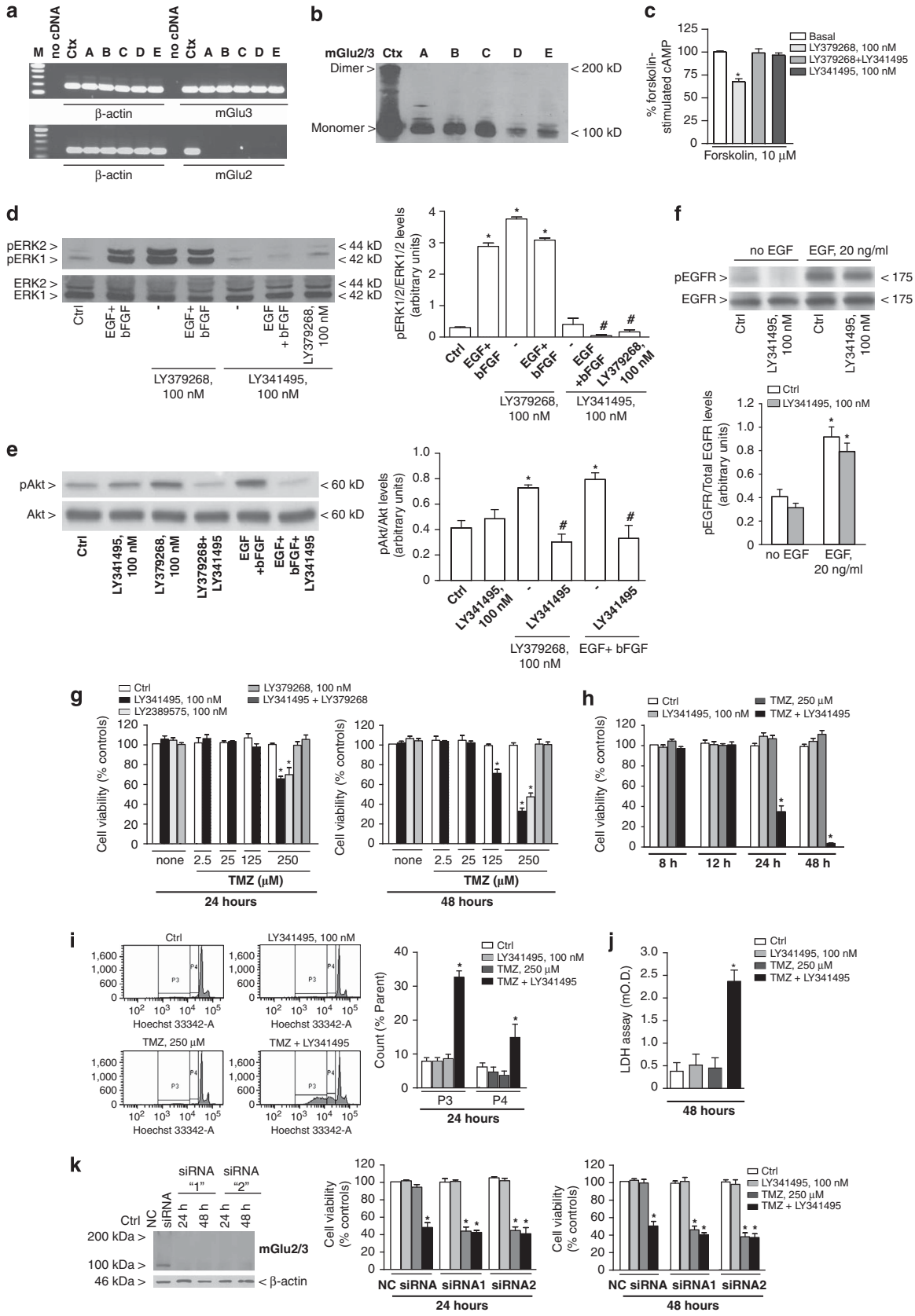
a
M no cDNA Ctx A B C D E no cDNA Ctx A B C D E
β-actin
mGlu3
β-actin
mGlu2
b
mGlu2/3 Ctx A B C D E
Dimer >
Monomer >
< 200 kD
< 100 kD
c
% forskolin-stimulated cAMP
Basal
LY379268, 100 nM
LY379268+LY341495
LY341495, 100 nM
Forskolin, 10 μM
d
pERK2 >
pERK1 >
ERK2 >
ERK1 >
< 44 kD
< 42 kD
Ctrl
EGF+ bFGF
EGF + bFGF
LY379268, 100 nM
LY379268, 100 nM
LY341495, 100 nM
pERK1/2/ERK1/2 levels (arbitrary units)
e
pAkt >
Akt >
< 60 kD
Ctrl
LY341495, 100 nM
LY379268, 100 nM
LY379268+ LY341495
EGF +bFGF
EGF+ bFGF+ LY341495
pAkt/Akt levels (arbitrary units)
LY379268, 100 nM
EGF+ bFGF
f
no EGF
EGF, 20 ng/ml
pEGFR >
EGFR >
< 175 kD
Ctrl
LY341495, 100 nM
pEGFR/Total EGFR levels (arbitrary units)
no EGF
EGF, 20 ng/ml
g
Ctrl
LY341495, 100 nM
LY2389575, 100 nM
LY379268, 100 nM
LY341495 + LY379268
Cell viability (% controls)
none 2.5 25 125 250
TMZ (μM)
24 hours
48 hours
h
Ctrl
LY341495, 100 nM
TMZ, 250 μM
TMZ + LY341495
8 h 12 h 24 h 48 h
i
Ctrl
LY341495, 100 nM
TMZ, 250 μM
TMZ + LY341495
Hoechst 33342-A
Count (% Parent)
P3 P4
24 hours
j
LDH assay (mO.D.)
48 hours
k
siRNA "1"
siRNA "2"
Ctrl
NC siRNA
24 h 48 h 24 h 48 h
200 kDa >
100 kDa >
46 kDa >
mGlu2/3
< β-actin
Cell viability (% controls)
NC siRNA siRNA1 siRNA2
24 hours
48 hours

clones). At least in clone E, treatment with LY341495 also reversed the increase in phospho-ERK1/2 and phospho-Akt levels induced by epidermal growth factor (EGF) and basic fibroblast growth factor (bFGF) (Figures 2d and e). LY341495 did not affect EGF receptor (EGFR) autophosphorylation in response to EGF (Figure 2f), suggesting that the drug had no direct off-target effects on EGFRs. Thus, these data suggest that endogenous activation of mGlu3 receptors has a permissive role on the stimulation of the MAPK and PtdIns-3-K pathways by mitogens.

GSCs were treated with temozolomide, a DNA-alkylating agent, which is widely used in the adjuvant chemotherapy of malignant gliomas.[14] Temozolomide (2.5–250 μM) did not affect cell viability when applied alone, but became toxic when combined with LY341495 and (3*S*)-1-(5-bromopyrimidin-2-yl)-N-(2,4-dichlorobenzyl)pyrrolidin-3-amine methanesulfonate hydrate (LY2389575), two drugs that block mGlu3 receptors. The mGlu2/3 receptor agonist, LY379268, was inactive on its own, but reversed the permissive action of LY341495 on temozolomide toxicity (Figures 2g–j and Supplementary Figure 2). siRNA-induced knockdown of mGlu3 receptors also enabled temozolomide toxicity, and the antagonist LY341495 did not further amplify toxicity in cells deprived of mGlu3 receptors (Figure 2k). These data indicate that activation of mGlu3 receptors by endogenous glutamate (extracellular glutamate concentrations: 4–10 μM; $n=6$) restrains the toxic action of temozolomide, and that GSCs become sensitive to temozolomide only if mGlu3 receptors are blocked or deleted.

Searching for the underlying mechanism(s), we treated GSCs with molecules that interfere with the three major signaling pathways activated by mGlu3 receptors, that is, inhibition of adenylyl cyclase activity, activation of the MAPK pathway, and activation of the PtdIns-3-K pathway. The cell-permeable cAMP analog, 8-Br-cAMP (1 mM), did not affect the synergism between mGlu3 receptor blockade and temozolomide, and the MAPK kinase inhibitor, UO126 (30 μM), had little, if any, effect on temozolomide toxicity (Figure 3a). In contrast, the PtdIns-3-K inhibitor, 2-(4-morpholinyl)-8-phenyl-4*H*-1-benzopyran-4-one hydrochloride (LY294002), had a permissive action on temozolomide toxicity, thus mimicking the effect of mGlu3 receptor blockade. The actions of LY294002 and LY341495 were less than additive (Figure 3a), suggesting that mGlu3 receptor blockade facilitates cytotoxicity by limiting the activation of the PtdIns-3-K pathway. This hypothesis was supported by the use of GSCs expressing a constitutively active form of the PtdIns-3-K substrate, Akt[15] (see Supplementary Figure 3). In these cells, in which the PtdIns-3-K pathway was active in spite of mGlu3 receptor blockade, the synergism between LY341495 and temozolomide was largely attenuated (Figure 3b). We extended the study to signaling pathways that lie downstream of Akt and are known to regulate viability and chemosensitivity of GSCs and glioma cells. Akt is known to activate nuclear factor-κB (NF-κB) by phosphorylating the IκB kinase,[16] and NFκB activation limits the proapoptotic activity of DNA-alkylating agents in glioma cells.[17] Here, treatment with temozolomide activated NF-κB, as shown by increased levels of IκB phosphorylation. This effect was reversed by LY341495 or by the PtdIns-3-K inhibitor, LY294002 (Figures 3c and d). The specific NF-κB inhibitor, 4-methyl-*N*1-(3-phenyl-propyl)-benzene-1,2-diamine (JSH-23),[18] enabled temozolomide toxicity and occluded the permissive action of LY341495 in GSCs (Figure 3e). Similar effects were obtained with salicylic acid (Supplementary Figure 4), which also inhibits NF-κB.[19] As opposed to LY341495, JSH-23 could still enhance temozolomide toxicity in GSCs expressing the constitutively active form of Akt (Figure 3f), indicating that NF-κB lies downstream of Akt in the pathway that restrains temozolomide toxicity. Akt also regulates the mammalian target of rapamycin (mTOR), which promotes mRNA translation and protein synthesis by phosphorylating p70 S6 kinase and 4E-BP1.[20] mTOR supports the survival of glioblastoma cells,[20] and inhibitors of the Akt/mTOR pathway are under development for the treatment of malignant gliomas.[21] Here, however, the selective mTOR inhibitor, rapamycin, did not mimic, but rather abolished the permissive action of mGlu3 receptor blockade on temozolomide toxicity (Supplementary Figure 5).

mGlu3 receptors support MGMT expression in cultured human GCSs challenged with temozolomide. We examined whether the permissive effect of mGlu3 receptor blockade was specific for temozolomide or could be extended to other chemotherapeutic agents. GSCs grown under proliferating conditions were treated with etoposide, irinotecan, the irinotecan metabolite, 7-ethyl-10-hydroxy-camptothecin (SN38), cisplatin, or paclitaxel alone or combined with LY341495. These treatments had no

Figure 2 Human GSCs express functional mGlu3 receptors and their inhibition enables the cytotoxic action of temozolomide (TMZ). RT-PCR analysis of mGlu2 and mGlu3 receptor mRNA in control mouse brain tissue (cerebral cortex (Ctx)) and in all GSC clones (A–E) is shown in (**a**). Immunoblot analysis of mGlu2/3 receptors in shown in (**b**). We used an antibody that recognizes a C-terminus epitope common to mGlu2 and mGlu3 receptors. Inhibition of forskolin-stimulated cAMP formation by the mGlu2/3 receptor agonist, LY379268, in GSC clone 'E' is shown in (**c**). Values are means ± S.E.M. of 4–5 determinations. $P<0.05$ *versus* all other groups (one-way analysis of variance (ANOVA) + Tukey's *t*-test). Activation of the MAPK and the PtdIns-3-K pathways by LY379268 or mitogens in the absence or presence of LY341495 is shown in (**d**) and (**e**), respectively. Densitometric values are means ± S.E.M. of four determinations. $P<0.05$ *versus* controls (Ctrl) (*), or *versus* the corresponding values obtained in the absence of LY341495 ($^{\#}$) (one-way ANOVA + Tukey's *t*-test). Phosphorylation of EFGR induced by EGF in the absence or presence of LY341495 is shown in (**f**). GSCs of clone E were starved for 24 h and then plated in 35 mm Petri dishes (10^6 cells per dish) and cultured without mitogens for 12 h. Afterwards, cells were challenged with EGF (10 ng/ml) and/or LY341495 (100 nM) for 30 min. Values are means ± S.E.M. of four determinations. *$P<0.05$ (one-way ANOVA + Tukey's *t*-test) as compared with the corresponding values obtained in the absence of EGF. Toxicity was assessed in GSC of clone E treated with TMZ and/or the mGlu3 receptor antagonists, LY341495 and LY2389575. Data of the MTT assay are shown in (**g**, **h**). Values (means + S.E.M.) are expressed as percent of controls (Ctrl, no TMZ and no mGlu receptor ligands), and were calculated from the means of triplicates or quadruplicates from three to six individual culture preparations. *$P<0.05$ (one-way ANOVA + Tukey's *t*-test) *versus* the corresponding control values. Cytofluorimetric analysis of aneuploid DNA and lactate dehydrogenase (LDH) release are shown in (**i**) and (**j**), respectively. Values (means ± S.E.M.) were calculated from three individual culture preparations. *$P<0.05$ (one-way ANOVA + Tukey's *t*-test) *versus* the respective control values or *versus* values obtained with LY341495 or TMZ alone. TMZ toxicity in GSCs deprived of mGlu3 receptors is shown in (**k**). mGlu3 receptor knockdown in response to small interfering RNA (siRNA) treatment is shown in the immunoblot. NC siRNA, non-coding siRNA. Values (means ± S.E.M.) were calculated from three to four individual cultures. *$P<0.05$ (one-way ANOVA + Tukey's *t*-test) *versus* the respective controls

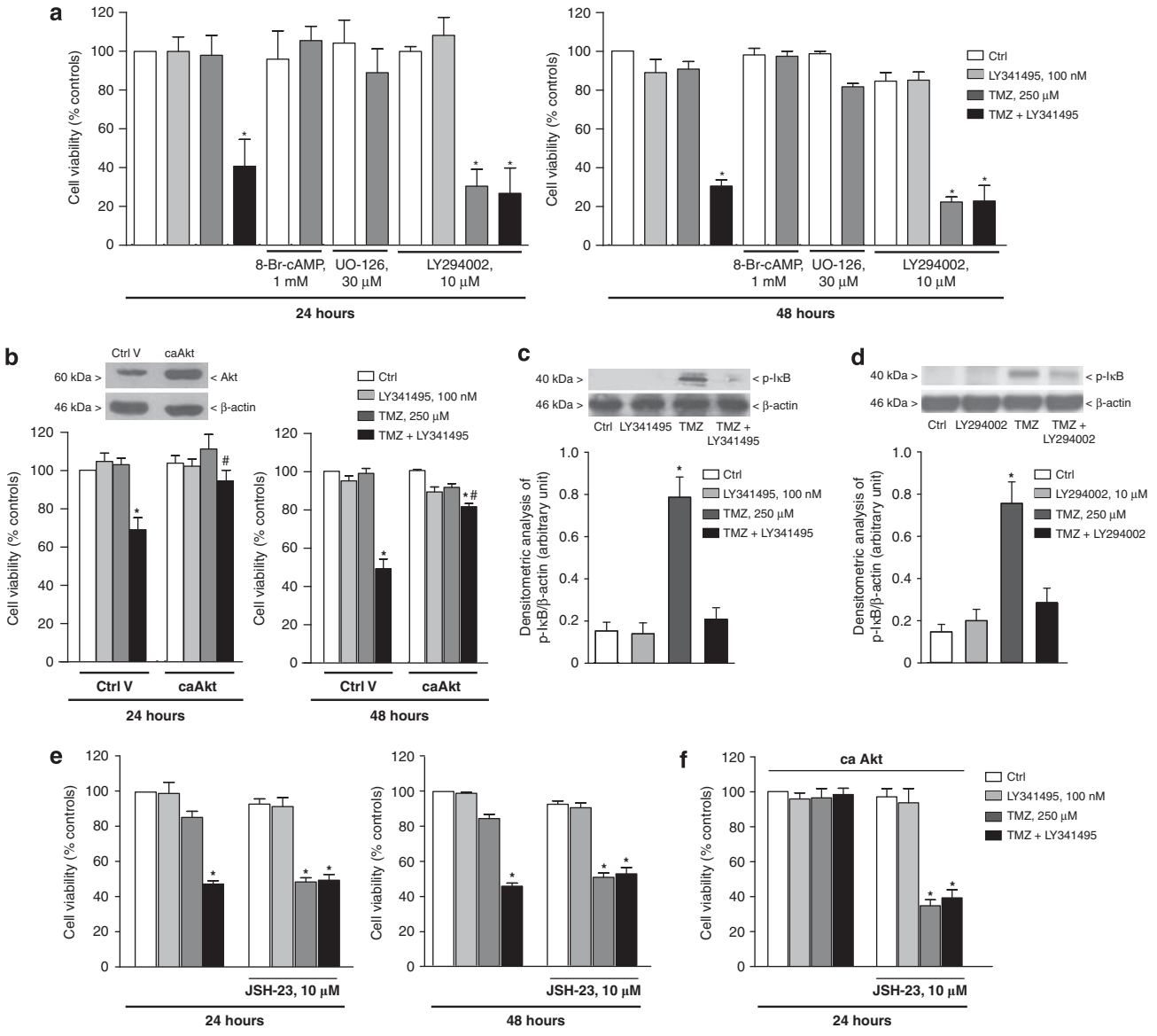

Figure 3 mGlu3 receptors restrain temozolomide (TMZ) toxicity by activating the PtdIns-3-K/Akt/NF-κB pathway. TMZ toxicity in GSCs treated w/wo LY341495, 8-bromo-cyclic AMP (8-Br-cAMP) or inhibitors of the MAPK and the PtdIns-3-K pathways is shown in (**a**). Values (means ± S.E.M.) are expressed as percent of the first control bar (see legend of Figure 1) were calculated from three to four individual culture preparations. $^*P<0.05$ (one-way analysis of variance (ANOVA) + Tukey's *t*-test) *versus* the respective controls (Ctrl). Data obtained with GSCs expressing a constitutively active form of Akt (caAkt) and treated with TMZ and/or LY341495 are shown in (**b**). The immunoblot shows the expression of Akt in GSC transfected with a control vector (Ctrl V) or with a vector encoding caAkt. Values (means ± S.E.M.) were calculated from three individual culture preparations. $P<0.05$ (one-way ANOVA + Tukey's *t*-test) *versus* the respective controls (*) or *versus* TMZ + LY341495 (#). Phosphorylation of IκB in response to TMZ in the absence or presence of LY341495 or LY294002 is shown in (**c**) and (**d**), respectively. Values are means + S.E.M. from four determinations. $^*P<0.05$ (one-way ANOVA + Tukey's *t*-test) *versus* the respective controls. The action of the NF-κB inhibitor, JSH-23, is shown in (**e**) and (**f**). In (**f**), GSCs were transfected with the vector encoding caAkt. Values (means + S.E.M.) were calculated from three individual culture preparations. $^*P<0.05$ (one-way ANOVA + Tukey's *t*-test) *versus* the respective controls. UO-126, 1,4-diamino-2,3-dicyano-1,4-bis[2-aminophenylthio]butadiene

significant effect on GSC viability (Figure 4 and Supplementary Figure 6), suggesting that mGlu3 receptors selectively control responses to temozolomide. The clinical efficacy of temozolomide is limited by the DNA-repairing enzyme, O^6-methylguanine-DNA methyltransferase (MGMT), which removes DNA adducts generated by alkylating agents.[22] Our GSC clones expressed MGMT. Treatment of GSCs with temozolomide alone increased MGMT mRNA levels at 3 h and slightly reduced MGMT protein levels at 24 and 48 h as a result of the loss of protein associated with DNA repair.[22] The transcript of MGMT failed to increase, and MGMT protein levels were markedly reduced when temozolomide was combined with the mGlu3 receptor antagonist, LY341495 (Figures 5a and b and Supplementary Figure 7). Again, the action of LY341495 was mimicked by an siRNA-induced knockdown of mGlu3 receptors (Figure 5c), by the PtdIns-3-K inhibitor, LY294002 (Figure 5d), and by the NF-κB inhibitor, JSH-23 (Figure 5e).

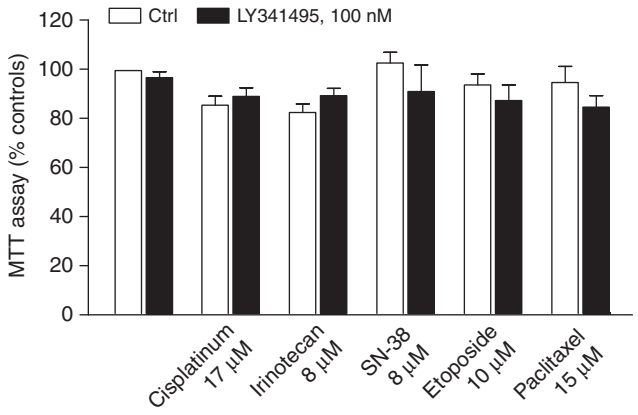

Figure 4 mGlu3 receptor blockade with LY341495 fails to influence the cytotoxic activity of non-alkylating anticancer drugs on GSCs. GSCs of clone E were treated for 48 h with cisplatinum, irinotecan, SN38, etoposide, and paclitaxel in the presence or absence (Ctrl) of LY341495. Values (means + S.E.M.) were calculated from four to six individual culture preparations

Treatment of GSCs with temozolomide increased the binding of NF-κB on two responsive elements of the MGMT promoter by about four- to fivefold. This effect was abolished by LY341495, which was inactive on its own (Figure 5f). Finally, the permissive action of LY341495, LY294002, or JSH-23 was no longer seen in GSCs overexpressing MGMT (Figures 6a–c), demonstrating that the synergism between mGlu3 receptor blockade and temozolomide was mediated by the inhibition of MGMT expression. This hypothesis was supported by the evidence that treatment with the MGMT inhibitor, O^6-benzylguanine,[23,24] enabled temozolomide toxicity (Figure 6d). Taken together, these data suggest that mGlu3 receptors restrain temozolomide toxicity by supporting the induction of MGMT by temozolomide via an intracellular signaling pathway that sequentially involves PtdIns-3-K and NF-κB (see model in Figure 6e).

Pharmacological blockade of mGlu3 receptors reduces tumor growth in mice infused with GCSs. To strengthen the biological significance of our findings, we performed *in vivo* studies on mice implanted with human GSCs in the brain parenchyma. Cells engineered to express the green fluorescent protein (GFP) were implanted into the left caudate nucleus of nude mice (5×10^5 cells/5 μl/5 min). We carried out two sets of experiments, each with four groups of 10 mice. All mice were subcutaneously implanted with osmotic minipumps releasing LY341495 (3 mg/kg per day for 28 days) or saline. At the same time, mice received three injections of temozolomide (70 mg/kg, intraperitoneally) or vehicle every other day during the first week following minipump implantation. In one experiment, mice received drug treatments 15 days after GSC implantation and were killed 30 days later (i.e. 45 days after cell implantation) (Figure 7a). Alternatively, mice were treated with drugs 45 days after GSC implantation and killed 30 days later (i.e. 75 days after cell implantation) (Figure 7b). Control mice, that is, mice implanted with a minipump releasing saline and receiving vehicle intraperitoneally, showed the presence of GFP^+ cells bearing the typical morphology of glioma cells, as assessed by hematoxylin–eosin staining. In mice killed 45 days after cell implantation, tumor cells were confined to the medial portion of the caudate nucleus close to the wall of the lateral ventricle (Figure 7a, a1, and a2). In mice killed at 75 days, tumor cells formed an infiltrating mass in the ipsilateral caudate nucleus and, in most of the animals, they spread to the ipsilateral septum and to the ipsi- and contralateral portion of the corpus callosum (Figure 7b and b1–3). Using this treatment paradigm, we did not see any significant effect of LY341495 *per se* on tumor growth. Treatment with temozolomide alone was also ineffective. In contrast, a combined treatment with temozolomide and LY341495 significantly reduced tumor growth (Figures 7a2 and b3 and Supplementary Figure 8), in good agreement with *in vitro* data.

Low levels of mGlu3 receptor mRNA in tumor specimens are predictive of long survival in patients with GBM receiving adjuvant temozolomide. We searched for an association between expression of mGlu3 receptors in tumor samples and survival of patients with GBM undergoing surgery followed by radiotherapy and adjuvant temozolomide. The transcript of mGlu3 receptors was measured by quantitative PCR in selected regions of the tumor in a cohort of 87 patients (Supplementary Table 1). 'Normal' mGlu3 receptor mRNA levels were defined as those measured in autoptic brain samples with no histological abnormalities ($n = 20$). Levels of mGlu3 receptor mRNA below the normal range were detected in 42 GBMs (48.3%), whereas in 45 cases (51.7%) mRNA levels either fell within the normal range ($n = 14$) or were higher than normal ($n = 31$) (Figure 8a). The Kaplan–Meier analysis of OS on mGlu3 receptor mRNA expression predicted a prolonged OS ($P < 0.0001$; HR: 3.129; 95% CI: 1.808–5.414) in the group of patients with mGlu3 receptor mRNA expression below the normal range (Figure 8b). Interestingly, all five patients who survived longer than 36 months harbored tumors with mGlu3 receptor mRNA below the normal range. On multivariate analysis, Karnofsky performance score, Ki-67, and mGlu3 receptor mRNA emerged as independent predictors for OS ($P = 0.000671$, 0.000504, and 0.001374, respectively) (Supplementary Table 2). We also stratified patients for mGlu3 receptor expression and the methylation state of MGMT promoter. The group with low mGlu3 receptor mRNA levels and methylated MGMT promoter showed a significantly higher OS as compared with the group with low mGlu3 receptor mRNA and unmethylated MGMT promoter ($P = 0.0020$). Patients with high/'normal' mGlu3 receptor mRNA and methylated MGMT promoter showed a low OS, regardless of the methylation state of MGMT promoter (Figure 8c).

Discussion

The glutamate released from glioma cells appears to play a central role in the malignant phenotype of gliomas by causing excitotoxic neurodegeneration and epileptic seizures via the activation of neuronal glutamate receptors,[25–27] and by regulating glioma cell proliferation and perivascular glioma invasion via the autocrine/paracrine activation of AMPA (2-amino-3-(3-hydroxy-5-methyl-isoxazol-4-yl)propanoic acid)

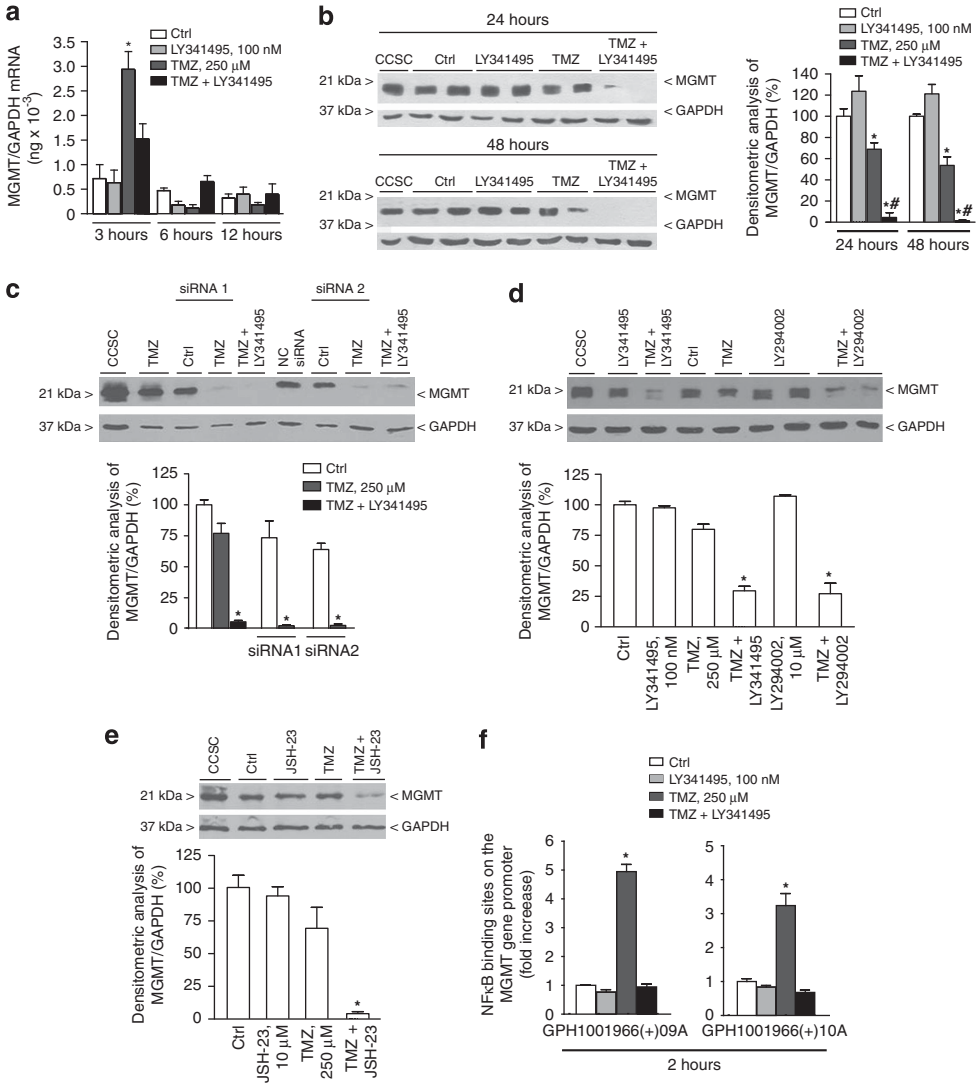

Figure 5 mGlu3 receptor blockade enables temozolomide (TMZ) toxicity by inhibiting MGMT expression in GSCs. Real-time PCR analysis of MGMT expression at three different times (3, 6, and 12 h) in cultured GSCs treated with LY341495 and TMZ alone or in combination is shown in (**a**). Values are means ± S.E.M. of three determinations. *$P<0.05$ *versus* controls (Ctrl) (one-way analysis of variance (ANOVA) + Tukey's *t*-test). Western blot analysis of MGMT protein expression after administration of LY341495 and TMZ alone or in combination is shown in (**b**). Colon cancer stem cells (CCSCs) were used as positive controls for the expression of MGMT. Densitometric values are means ± S.E.M. of three determinations. $P<0.05$ (one-way ANOVA + Tukey's *t*-test) *versus* the respective controls or LY341495 alone (*), or *versus* TMZ alone ($^{\#}$). MGMT protein levels after small interfering RNA (siRNA)-induced knockdown of mGlu3 receptors is shown in (**c**). Values are means ± S.E.M. of three determinations. *$P<0.05$ (one-way ANOVA + Tukey's *t*-test) *versus* the respective controls. MGMT protein levels in GSCs treated with the PtdIns-3-K inhibitor, LY294002, or with the NF-κB inhibitor, JSH-23, are shown in (**d**) and (**e**), respectively. Values are means ± S.E.M. of three to six determinations. *$P<0.05$ (one-way ANOVA + Tukey's *t*-test) *versus* the respective controls. NF-κB binding to MGMT promoter regions in GSCs treated with TMZ and/or LY341495 is shown in (**f**). Values are means ± S.E.M. of nine determinations from three independent ChIP experiments. *$P<0.05$ (one-way ANOVA + Tukey's *t*-test) *versus* all other values. GAPDH, glyceraldehyde 3-phosphate dehydrogenase

receptors.[28–30] Our data disclose a new function of glutamate in regulating the biology of GSCs. The amount of glutamate released from GSCs in culture (extracellular concentrations = 4–10 μM) was sufficient to activate mGlu3 receptors, which were expressed and functional in all our GSC clones (EC_{50} values for glutamate at mGlu3 receptors are reported in Schoepp *et al.*[31].). All our GSC clones were highly resistant to the cytotoxic activity of temozolomide unless the mGlu3 receptor was blocked. Inhibition of PtdIns-3-K and its effector pathways could also facilitate temozolomide toxicity, as expected.[32] What is novel here is that PtdIns-3-K was tightly regulated by mGlu3 receptors, and that receptor blockade was sufficient to suppress temozolomide-induced MGMT expression and to enable temozolomide toxicity. This suggests that, at least under our conditions, other endogenously active receptors coupled to PtdIns-3-K could not rescue temozolomide-induced MGMT expression when mGlu3 receptors were blocked. NF-κB, which is activated by the PtdIns-3-K/Akt pathway,[15] is one of the strongest inducers of MGMT expression. In recombinant cells, NF-κB/p65 homodimers enhance MGMT expression sevenfold more than AP1/c-jun, and, remarkably, induction of MGMT by NF-κB is unaffected by the methylation state of the MGMT gene promoter.[33] We have shown that mGlu3 receptor blockade

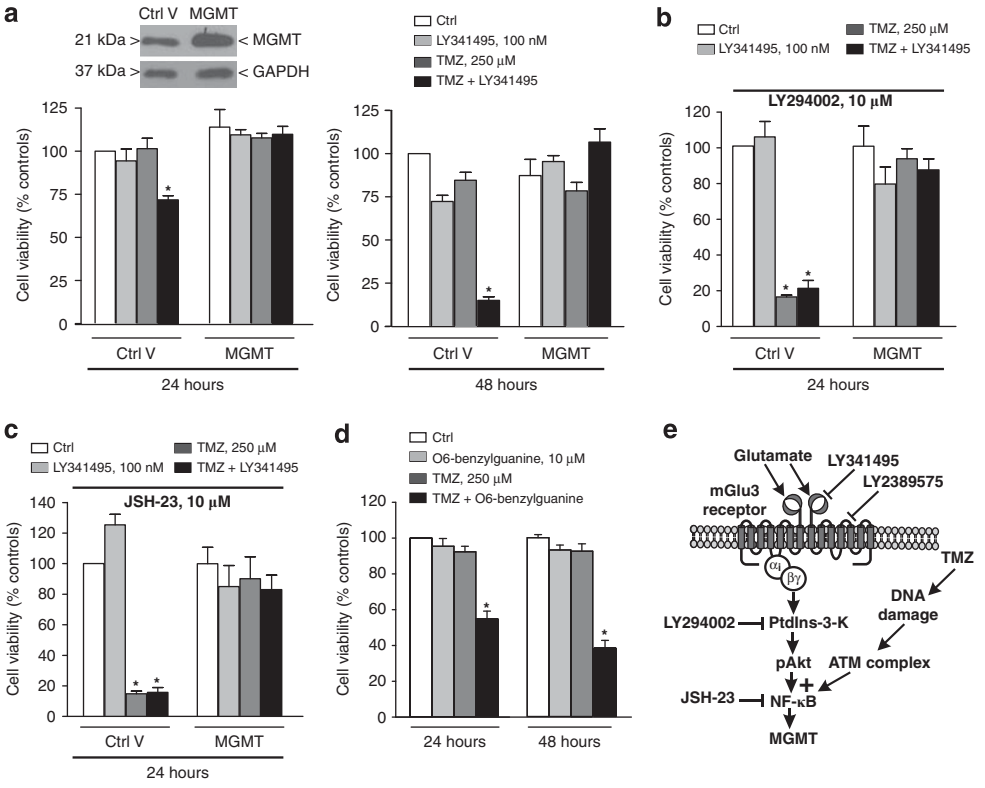

Figure 6 Suppression of temozolomide (TMZ)-induced MGMT expression mediates the permissive role of mGlu3 receptor blockade on TMZ toxicity in GSCs treated with a control vector (Ctrl V) or with a vector encoding human MGMT and exposed to LY341495, LY294002, or JSH-23 is shown in (**a**), (**b**), and (**c**), respectively. Values (means + S.E.M.) are expressed as percent of the first control bar (see above) and were calculated from three individual culture preparations. $^*P<0.05$ (one-way analysis of variance (ANOVA) + Tukey's *t*-test) *versus* the respective controls. TMZ toxicity in GSCs co-treated with the MGMT inhibitor, O^6-benzylguanine, is shown in (**d**). Values (means + S.E.M.) were calculated from three individual culture preparations. $^*P<0.05$ (one-way ANOVA + Tukey's *t*-test) *versus* the respective controls. A schematic model showing the mechanism by which activation of mGlu3 receptors supports TMZ-induced MGMT expression and restrains TMZ toxicity is shown in (**e**). ATM, *A*taxia *T*elangiectasia *M*utated; GAPDH, glyceraldehyde 3-phosphate dehydrogenase

substantially reduced NF-κB binding to the MGMT gene promoter in GCSs treated with temozolomide, raising the interesting possibility that activation of mGlu3 receptors may support MGMT expression even if the MGMT promoter is hypermethylated. Two sets of data are consistent with this hypothesis: (i) treatment with LY341495 inhibited temozolomide-induced MGMT expression and enabled temozolomide toxicity also in GSCs of clone 'A', which derived from a tumor in which the MGMT gene promoter was methylated; and (ii) the survival of temozolomide-treated patients with high levels of mGlu3 receptor mRNA in the tumor was totally unaffected by the methylation state of the MGMT promoter (see Figure 8c). Our data also suggest that hypermethylation of the MGMT promoter is a positive predictor of survival only in patients with low mGlu3 receptor expression in tumor specimens. The dependency of MGMT on the expression levels of mGlu3 receptors might help to explain the controversial data on the correlation between MGMT promoter methylation and patients' survival.[34–40]

Our data may pave the way to a new strategy in the pharmacological treatment of malignant gliomas because mGlu3 receptor antagonists could be added to temozolomide or other DNA-alkylating agents for the optimization of adjuvant chemotherapy. The evidence that a combined treatment with temozolomide and LY341495 was still efficacious in restraining tumor growth when initiated 45 days after cell implantation in mice is particularly promising for translation into medical practice because of the long interval between onset and treatment of malignant gliomas.

As opposed to small-molecule inhibitors of intracellular enzymes or transcription factors that regulate chemoresistance, such as PtdIns-3-K or NF-κB, mGlu3 receptor antagonists are expected to be safe and well tolerated, as shown by all clinical trials with mGlu receptor ligands in neurological and psychiatric disorders.[13] Accordingly, we did not see signs of systemic toxicity or motor impairment in mice treated with 3 mg/kg per day of LY341495, and, in acute experiments, naive mice survived to doses of LY341495 as high as 300 mg/kg, intraperitoneally (not shown).

In conclusion, we have demonstrated that the mGlu3 receptor, a particular type of G-protein-coupled receptor activated by glutamate, restrains temozolomide toxicity by exerting a permissive role on temozolomide-induced MGMT expression in GSCs. We propose a hypothetical model in which the convergence of at least two intracellular pathways is required for NF-κB activation and MGMT induction in response to temozolomide. One of this pathway might be directly linked to DNA damage caused by temozolomide via the activation of the ataxia–telangiectasia-mutated protein complex or other mechanisms.[41–44] The other pathway is

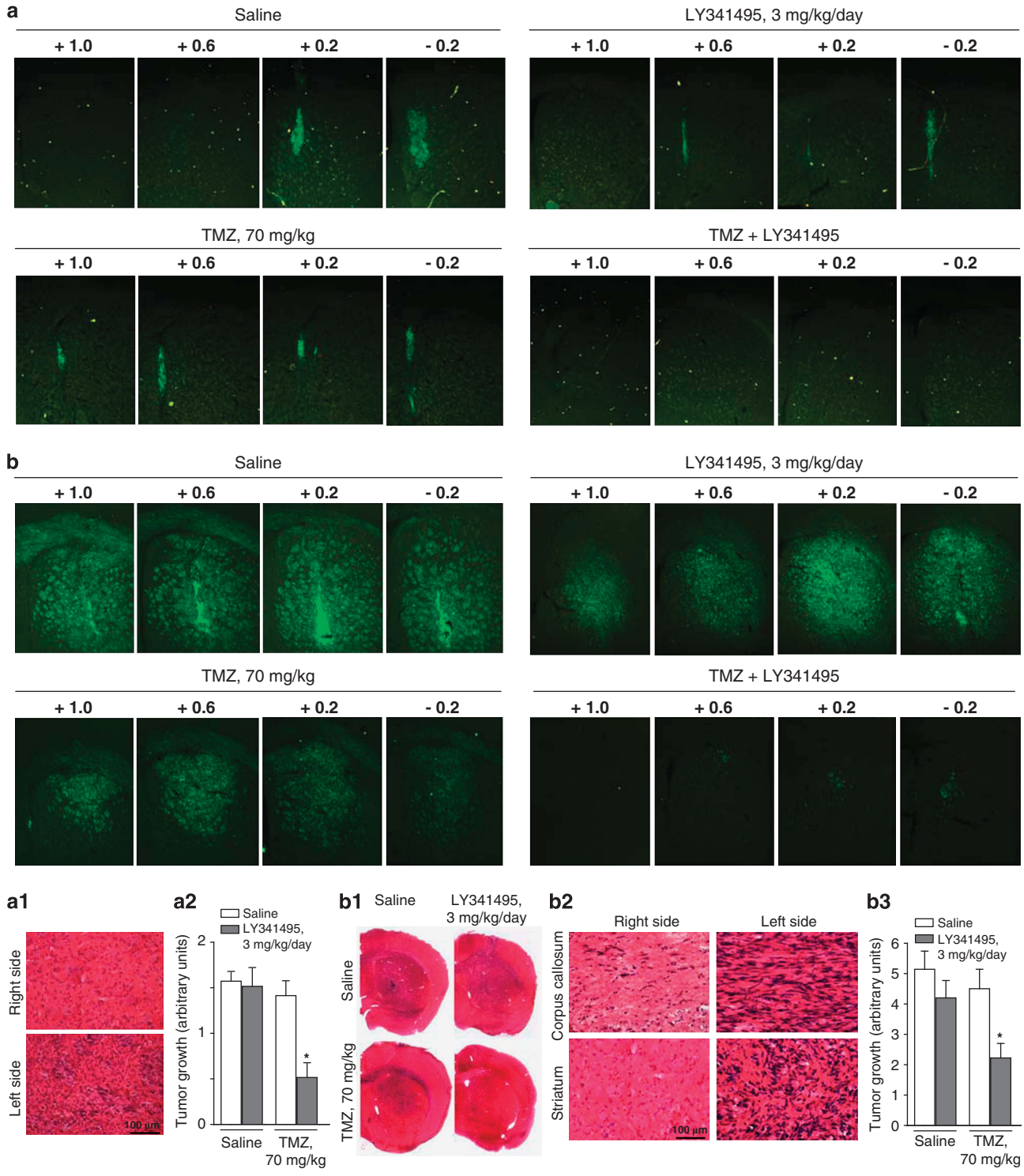

Figure 7 Combined treatment with temozolomide (TMZ) and LY341495 inhibits tumor growth in mice implanted with GSCs into the brain parenchyma. In (**a**), (**a1**), and (**a2**), mice were implanted with osmotic minipumps releasing LY341495, 3 mg/kg per day for 28 days, 15 days after injection of GSCs into the left caudate nucleus. TMZ was injected intraperitoneally once daily every other day for 1 week starting from the day of minipump implantation. Mice were killed 30 days following minipump implantation (i.e. 45 days after GSC injection). Representative images showing the presence of GFP^+ GSCs in the injection site are in (**a**). Numbers from $+1.0$ to -0.2 refer to the distance (in mm) from bregma. The histological features of the tumor are shown by hematoxylin/eosin staining in (**a1**). Data of tumor growth (see Materials and Methods for the scoring at 45 days) are shown in (**a2**). Values are means ± S.E.M. of 8–10 mice per group. $^*P<0.05$ (one-way analysis of variance (ANOVA) + Tukey's *t*-test) *versus* all other values. In (**b**), (**b1**), (**b2**), and (**b3**), experiments were carried out as in (**a**), with the difference that drug treatment started 45 days after GSC injection, and mice were killed 30 days later (75 days after GSC injection). Representative images of the injected site are shown in (**b**). The histology of the tumor is shown in (**b1**) and (**b2**). Data of tumor growth (see Materials and Methods for the scoring at 75 days) are shown in (**b3**), where data are means ± S.E.M. of 6–8 mice per group. $^*P<0.05$ (one-way ANOVA + Tukey's *t*-test) *versus* all other values

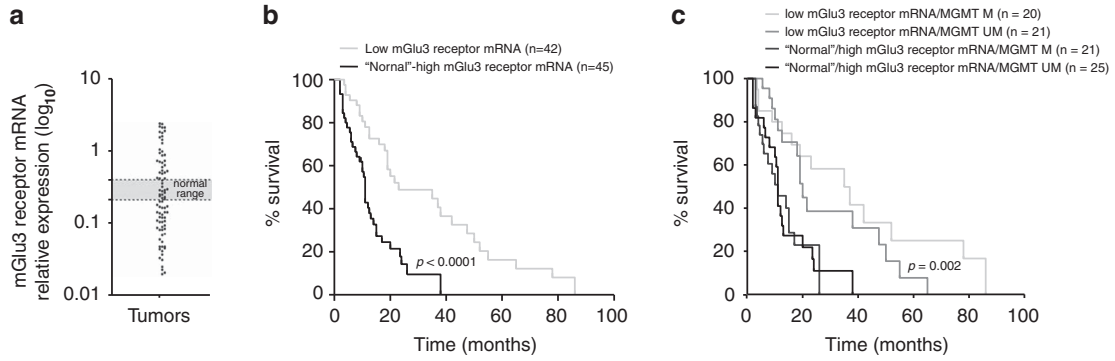

Figure 8 Inverse relation between tumor and mGlu3 receptor mRNA and OS in patients with GBM tumors treated with temozolomide. A scattered diagram plotting the mGlu3 receptor mRNA levels on GBM tumors ($n = 87$) is shown in (**a**). A 'normal' range is defined on the basis of values obtained from autoptic brains with no histological abnormalities ($n = 20$). Kaplan–Meier survival curves of GBM patients stratified by tumor mGlu3 receptor mRNA expression alone or mGlu3 receptor mRNA expression combined with the methylation state of MGMT promoter is shown in (**b**) and (**c**), respectively. MGMT M, methylated promoter of the MGMT gene promoter; MGMT UM = unmethylated promoter

activated by the endogenous glutamate acting at mGlu3 receptors and is mediated by PtdIns-3-K (see Figure 6e). Thus, glutamate, the major excitatory neurotransmitter in the CNS, is not only involved in the regulation of tumor invasion and cell proliferation but also acts as a critical regulator of the intracellular signaling pathways that mediate chemoresistance, thereby limiting the clinical efficacy of standard chemotherapy with DNA-alkylating agents.

Materials and Methods

Temozolomide, cisplatinum, irinotecan, etoposide, paclitaxel, 8Br-cAMP, and O^6-benzylguanine were purchased from Sigma-Aldrich (St. Louis, MO, USA). UO-126 was purchased from Promega (Milano, Italy). LY341495, LY379268, LY294002, and SN38 were purchased from Tocris Cookson Ltd (Bristol, UK). LY2389575 was kindly provided by Eli Lilly and Company (Indianapolis, IN, USA) to FN. JSH-23 and sodium salicylate were purchased from Santa Cruz Technology (Santa Cruz, CA, USA).

Cultures of human GSCs. Human GSCs were derived from five adult human glioblastoma bioptic samples (after obtaining informed consent) classified according to the guidelines of the World Health Organization. In three of these samples, giving raise to GSC clones 'B', 'D', and 'E', the MGMT gene promoter was unmethylated. In the glioblastoma sample giving raise to GSC clone 'A', the MGMT gene promoter was methylated. We have no information on the methylation state of the MGMT gene promoter in the remaining glioblastoma sample giving raise to clone 'C'. Undifferentiated GBM stem cells were obtained through mechanical dissociation of the tumor tissue and cultured in a serum-free medium. Briefly, tissue chunks were collected in Dulbecco's modified Eagle medium (DMEM)/F12, homogenized through vertical blade cuts, and then centrifuged for 3 min at 1000 r.p.m.; the pellet was mechanically dissociated to a single-cell suspension. Cells were re-suspended in serum-free enriched DMEM/F12 medium in the presence of 10 ng/ml of human recombinant EGF and 20 ng/ml of human recombinant bFGF, and plated in 75 cm^2 culture flask (Falcon BD, Franklin Lakes, NJ, USA). Under these culture conditions, cells proliferated and aggregated into tumor spheres, and maintained an undifferentiated state, as indicated by morphology and expression of the stem cell markers. At 1 week after plating, primary tumor spheres were collected, mechanically dissociated, and re-plated under the same culture conditions to eliminate short-term dividing precursors.

Immunocytochemical analysis of Musashi1 and Sox-2. Cells were fixed with 4% paraformaldehyde and stained with antibodies directed against Sox-2 (R&D Systems, Minneapolis, MN, USA; 1 : 200) or MMusashi1 (R&D Systems; 1 : 200). As secondary antibodies, goat anti-rabbit fluorescein isothiocyanate-conjugated IgG (Chemicon, Temecula, CA, USA; 1 : 100) were used. Nuclei were counterstained with 4,6-diamidino-2-phenylindole (DAPI) (Vectashield mounting medium with DAPI; Vector Laboratories, Burlingame, CA, USA).

RT-PCR analysis of mGlu2 and mGlu3 receptor mRNA. Reverse transcriptase-polymerase chain reaction (RT-PCR) analysis was performed using the following primers: mGlu2 – forward, 5′-AGCACCTTTGCTGGTTAGGA-3′; reverse, 5′-ACCCGAGCTCTTCAGACTCA-3′; mGlu3 – forward, 5′-GCAGTTTGT CTTGGTCAGCA-3′; reverse, 5′-AACACACCCTTGGTCAAAGC-3′; β-actin – forward, 5′-AGCACTGTGTTGGCGTACAG-3′; reverse, 5′-AGAGCTACGAGCT GCCTGAC-3′.

All transcripts obtained spanned around 100 bp.

Western blot analysis. Cells were lysed using a Triton X-100 lysis buffer (10 mM Tris-HCl, pH 7.4, 150 mM NaCl, 1% Triton X-100, 1 mM EDTA, 10% glycerol, 1 mM phenylmethylsulfonyl fluoride, 10 μg/ml leupeptin, 10 μg/ml aprotinin, 1 mM sodium orthovanadate, 50 mM sodium fluoride, and 10 mM β-glycerophosphate) for 15 min, and cell lysates were clarified by centrifugation (12 000 r.p.m. for 10 min). Proteins (40 μg) were separated by sodium dodecyl sulfate (SDS)-polyacrylamide gel electrophoresis, blotted onto nitrocellulose membranes, and probed with the following primary antibodies: rabbit polyclonal anti-mGlu2/3 receptor (Upstate Biotechnology, Lake Placid, NY, USA; 1 : 750); mouse monoclonal anti-phospho-ERK1/2 (Cell Signaling Technology, Danvers, MA, USA; 1 : 500), rabbit polyclonal anti-ERK1/2 (Santa Cruz Biotechnology, Tebu, France; 1 : 2000); rabbit polyclonal anti-phospho-Akt (Cell Signaling; 1 : 500); rabbit polyclonal anti-Akt (Cell Signaling; 1 : 1000); rabbit polyclonal anti-MGMT (Cell Signaling; 1 : 500); mouse monoclonal anti-β-actin (Sigma-Aldrich, St. Louis, MO, USA; 1 : 2500); rabbit polyclonal anti-phospho-Tyr1068-EGF receptor (EGFR) (Cell Signaling; 1 : 500); rabbit polyclonal anti-EGFR (Cell Signaling; 1 : 1000); mouse monoclonal anti-phospho-Ser32/Ser36-IκBα (Cell Signaling; 1 : 1000); rabbit polyclonal anti-phospho-Ser9-glycogen synthase kinase-3β (GSK3β) (Cell Signaling; 1 : 500); and rabbit polyclonal anti-GSK3β (Cell Signaling; 1 : 1000).

Measurement of extracellular glutamate levels. Analysis of glutamate in the medium of GSCs was performed by precolumn derivatization with *o*-phthalaldehyde and mercaptoethanol, followed by high-performance liquid chromatography with fluorescence detection. A measure of 10 μl sample aliquots were diluted with 0.1 M HCl and mixed with equal volumes of fluorescent reagent. The mixture was kept at room temperature for 1 min to derivatize the sample before being injected into the column by a 20 μl loop. The system utilized an autosampler 507 (Beckman Instruments Inc., Fullerton, CA, USA), a programmable solvent module 126 (Beckman Instruments Inc.), an analytical reverse phase C-18 column at 30 °C (Ultrasphere ODS 3 μm Spherical, 80 Å pore, 2 mm × 150 mm; Beckman Instruments Inc.), an RF-551 spectrofluorimetric detector (Shimadzu, Japan), and a computer running a Gold Nouveau software (Beckman Instruments Inc.). The excitation and emission wavelengths were set at 360 and 450 nm, respectively. The mobile phase consisted of: (A) 50 mM

sodium phosphate, pH 7.2, containing 10% methanol and (B) 50 mM sodium phosphate, pH 7.2, containing 70% methanol, at a flow rate of 0.3 ml/min. Gradient elution consisted of 98% A and 2% B initially for 10 min, was then increased to 98% B over 1 min, maintained for 1 min to elute other substances, and then returned to the initial conditions before running the next sample. From peak areas, culture medium concentrations of glutamate were calculated by the use of external standards.

Measurement of intracellular cyclic AMP levels. Cells were incubated in Krebs–Henseleit buffer containing 0.5 mM isobutylmethylxantine for 15 min at 37 °C under constant oxygenation. After the addition of forskolin and/or mGlu receptor ligands, the incubation was continued for 20 min. The reaction was stopped by the addition of an equal volume of ice-cold 0.8 N $HClO_4$. Samples were sonicated and centrifuged at low speed. After the addition of K_2CO_3, samples were centrifuged and supernatants used for assessment of cAMP by radioimmunoassay (GE Healthcare, Milano, Italy).

Assessment of cell viability

MTT assay: Cell viability was assessed by using the Cell Titer 96 Non-Radioactive Cell Proliferation Assay (Promega) according to the manufacturer's protocol. The assay is based on the reduction of 3-(4,5-dimethylthioazol-2-yl)-2,5-diphenyl tetrazolium bromide (MTT) to a colored formazan product, which is measured by spectrophotometry at a wavelength of 570 nm. Cells were plated in 96-well plates and treated as indicated. At the end of the treatments, cells were incubated at 37 °C in a 5% CO_2 incubator. Metabolically active cells were detected by adding 15 μl of dye solution to each well. After 1 h of incubation, 100 μl of solubilizing stop solution was added to the wells and the plates were read on a Multilabel Counter (Victor2; Perkin-Elmer, Waltham, MA, USA).

Cytofluorimetric analysis of aneuploid DNA: FACS analysis of DNA ploidy was carried out using a Coulter Elite flow cytometer after staining with propidium iodide (50 μg/ml) and treatment for 1 h with RNAse (100 μg/ml).

LDH release: Extracellular lactate dehydrogenase (LDH) activity was measured using a commercial kit (Roche Diagnostics SpA, Milano, Italy).

Assessment of NF-κB binding to responsive sequences in the MGMT promoter. Analysis of interaction between NF-κB and its two binding sites on the MGMT gene promoter was assessed by chromatin immunoprecipitation (ChIP). Crosslink between proteins and DNA was obtained with 1% formaldehyde, and ChIP was performed by a commercial kit (EpiTect ChIP One-Day Kit; SA Biosciences, Frederick, MD, USA) and a ChIP-grade NF-κB antibody (Cell Signaling Technology, Danvers, MA, USA; 1 : 500). For real-time PCR analysis of immunoprecipitated chromatin, we used two pairs of specific primers for the NF-κB binding sites on the MGMT gene promoter (GPH1001966(+)09A and GPH1001966(+)10A; SA Biosciences). Data, obtained with the $\Delta\Delta$Ct method for quantifying chromatin enrichment and normalized for input chromatin and background levels, were expressed as fold enrichment, and compared by measuring fold change in site occupancy between controls and treatments.

Silencing of mGlu3 receptors. mGlu3 receptor gene was silenced in human GBM stem cells by using a commercial kit supplied by Qiagen (Life Sciences, Milan, Italy). The following siRNAs were used: siRNA '1' (Hs_GRM3_1) – sense, 5′-GGUCCUUGUUGUAACUAAUTT-3′; antisense, 5′-AUUAGUUACAA CAAGGACCTA-3′; siRNA '2' (Hs_GRM3_4) – sense, 5′-GCGCCAAACUCAGU GAUAATT-3′; antisense, 5′-UUAAUCACUGAGUUUGGCGCTG-3′.

Cells were seeded at a density of 5×10^5 in 100 μl of culture medium in 96-well plates and incubated at 37 °C. After 24 h, a mix containing 150 ng of siRNA and 1 μl HiPerFect Transfection Reagent (Qiagen) was then added to the culture medium (final concentration 5 nM per well). Transfected and control cells were treated with temozolomide (250 μM) alone or in combination with LY341495 (100 nM). Cell viability was measured 24 and 48 h afterwards by MTT analysis.

Transient transfections. Transient transfections with the MGMT plasmid construct or the constitutively active Akt plasmid constructs were performed by the LipofectAMINE method (Invitrogen, Carlsbad, CA, USA) according to the manufacturer's instructions. GSCs were seeded at a density of 7.5×10^3 in 96-well plates and incubated, 1 day after plating, in Optimem with 0.5 μl of LipofectAMINE (Life Technologies Europe, Monza, Italy) reagent and 0.2 μg of plasmid construct for 4 h per well.

Evaluation of tumor growth in nude mice implanted with GFP$^+$ GBM stem cells into the brain. Experiments were performed in accordance with the Guidelines for Animal Care and Use of the National Institutes of Health. Male CD1 nude mice (Charles River, Calco, Italy; 20–22 g, body weight), and were kept under controlled conditions (temperature = 22 °C; humidity = 40%) on a 12-h light/dark cycle with food and water *ad libitum*. GSCs were engineered to express the GFP as described previously.[45] GFP$^+$ GSCs were stereotaxically implanted into the left caudate nucleus using the following coordinates: 0.6 mm anterior to bregma; 1.7 mm lateral to the midline; and 3.5 mm ventral from the surface of skull according to the atlas of Franklin and Paxinos, under ketamine (100 mg/kg, intraperitoneally)/xylazine (10 mg/kg, intraperitoneally) anesthesia. For limiting dilution assay, GCSs (0.01, 0.05, 0.1, or 0.5×10^6 cells/5 μl) were implanted at an infusion rate of 1 μl/min. The needle was left 5 min in place after cell infusion before being withdrawn. Animals were killed 3 months after GSC implantation. In another set of experiments, GCSs (0.5×10^6 cells/5 μl) were implanted at an infusion rate of 1 μl/min. The needle was left 5 min in place after cell infusion before being withdrawn. At 15 or 45 days after cell implantation, mice were implanted with osmotic minipumps (Alzet, releasing 250 nl/h per 28 days), filled with saline or LY341495 (3 mg/kg per day), and were treated with three injections of saline or temozolomide (70 mg/kg, intraperitoneally, every other day). Mice were killed 1 month later. Histological analysis was performed by hematoxylin/eosin staining. The growth of GSCs was assessed by fluorescence microscopy of GFP$^+$ GSCs according to the following score: 0, no GFP$^+$ GSCs; 1, presence of GFP$^+$ GSCs in the injection site; 2, presence of GFP$^+$ GSCs in the medial portion of the caudate nucleus close to the wall of the lateral ventricle; 3, presence of GFP$^+$ GSCs in about 50% of the left caudate nucleus; 4, presence of GFP$^+$ GSCs in the whole caudate nucleus and infiltrating the ipsilateral septum; 5, presence of GFP$^+$ GSCs in the whole caudate nucleus infiltrating the ipsilateral septum and corpus callosum; 6, presence of GFP$^+$ GSCs in the whole caudate nucleus infiltrating the ipsilateral septum and corpus callosum and a partial infiltration of the contralateral corpus callosum; and 7, presence of GFP$^+$ GSCs in the whole caudate nucleus infiltrating the ipsilateral septum and corpus callosum and a complete infiltration of the contralateral corpus callosum.

Patient population. We enrolled 87 adult patients who underwent craniotomy for resection of histologically confirmed GBM (World Health Organization grade IV) in the supratentorial compartment, and who had been treated postoperatively with adjuvant radiotherapy and temozolomide at Università Cattolica del Sacro Cuore (Rome, Italy). All patients provided written informed consent according to the Declaration of Helsinki (*BMJ* 1991; **302**: 1194) and to the research proposals approved by the Ethical Committee of the Università Cattolica del Sacro Cuore (Rome, Italy). Patients with secondary GBM were not included. Patients were 30 to 80 years old at the time of primary surgery (median age: 58 years); 57 were men and 30 women. All patients received radiotherapy to limited fields (2 Gy per fraction, once a day, 5 days a week, 60 Gy total dose) and adjuvant temozolomide after surgery.[7] To minimize contamination by normal cells, the tumor areas selected for DNA extraction contained at least 80% disease-specific cells. OS was calculated from the date of surgery to death or end of follow-up. Immunohistochemical patterns were established as reported previously.[45] The Ki-67 labeling index was defined as the percentage of positive nuclei of a total of 2000 tumor cells counted using an eyepiece grid. The positive nuclei were counted without prior knowledge of the patient prognosis-related information. The methylation state of the MGMT gene promoter was assessed as described previously.[46]

RNA extraction and analysis of mGlu3 receptor expression in human brain tissue. After being deparaffinized, three 10-μm-thick slides were digested overnight at 55 °C in 200 μl of TENS buffer 1 × (10 mM Tris, pH 7.4, 10 mM EDTA, 100 mM NaCl, 1% SDS) with 100 mg/ml proteinase K and RNA was then extracted by RNeasy mini kit (Qiagen), according to the manufacturer's protocol. We assessed the quantity and quality of the RNA spectrophotometrically (E260, E260/E280 ratio, spectrum 220–320 nm; Biochrom, Cambridge, UK) and by separation on an Agilent 2100 Bioanalyzer (Palo Alto, CA, USA). mGlu3 receptor mRNA levels were measured by using a One-Step qRT-PCR KAPA SYBR FAST kit (Kapa Biosystems, Boston, MA, USA) according to the manufacturer's protocol. The assay was performed on 67 GBMs and on 20 samples of human brain tissue showing no abnormalities at histology (normal control). Briefly, 100 ng of mRNA from each sample was reverse-transcribed and amplified in a 25 μl reaction volume with the following components: 12.5 μl of 2 × KAPA Sybr FAST qPCR master mix, 0.5 μl of KAPA RT mix (50 ×), 200 nM

forward and reverse primers, and DNase/RNase free water. The following primers were employed: mGlu3 receptor – forward, 5′-GCAGTTTGTCTTGGTCAGCA-3′; reverse, 5′-AACACACCCTTGGTCAAAGC-3′; β-actin – forward, 5′-AGCACTG TGTTGGCGTACAG-3′; reverse, 5′-AGAGCTACGAGCTGCCTGAC-3′.

Cycling conditions were: 10 min at 42 °C, 5 min at 95 °C, followed by 40 cycles each of 10 s at 95 °C and 30 s at 60 °C and 80 cycles of 55 + 0.5 °C per cycle for melting curve analysis in a iCycler-iQ multicolor Real-Time PCR detection system (Bio-Rad, Milan, Italy). β-Actin amplification was used as internal control. Specificity of products was assessed by direct sequencing, using the same primers used for PCR amplification. The average obtained for mGlu3 receptor was normalized to the average amount of β-actin for each sample to determine relative changes in mRNA expression (the ratio was calculated using the $2^{-\Delta Ct}$ method).

Conflict of Interest

The authors declare no conflict of interest.

Acknowledgements. mGlu2/3 receptor ligands were kindly provided by Eli Lilly and Company. The expression plasmid for β-catenin was provided by Dr. RT Moon (University of Washington, School of Medicine, Seattle, WA, USA). The pCDNA3/constitutively active Akt plasmid was kindly provided by Professor P Formisano, University of Naples 'Federico II', Italy. The pCDNA3/MGMT plasmid was kindly provided by Professor Alexandre Evrard, School of Pharmacy, Department of Toxicology, University of Montpellier I (Montpellier, France).

1. Wen PY, Kesari S. Malignant glioma in adults. *N Engl J Med* 2008; **359**: 492–507.
2. Van Meir EG, Hadjipanayis CG, Norden AD, Shu HK, Wen PY, Olson JJ. Exciting new advances in neuro-oncology. The avenue to a cure for malignant glioma. *CA Cancer J Clin* 2010; **60**: 166–193.
3. Galli R, Binda E, Orfanelli U, Cipelletti B, Gritti A, De Vitis S *et al.* Isolation and characterization of tumorigenic, stem-like neural precursors from human glioblastoma. *Cancer Res* 2004; **64**: 7011–7021.
4. Singh SK, Hawkins C, Clarke ID, Squire JA, Bayani J, Hide T *et al.* Identification of human brain tumor initiating cells. *Nature* 2004; **18**: 396–401.
5. Vescovi AL, Galli R, Reynolds BA. Brain tumor stem cells. *Nat Rev Cancer* 2006; **6**: 425–436.
6. Stiles CD, Rowitch DH. Glioma stem cells: a midterm exam. *Neuron* 2008; **58**: 832–846.
7. Pallini R, Ricci-Vitiani L, Banna GL, Signore M, Lombardi D, Todaro M *et al.* Cancer stem cell analysis and clinical outcome in patients with glioblastoma multiforme. *Clin Cancer Res* 2008; **14**: 8205–8212.
8. Eramo A, Ricci-Vitiani L, Zeuner A, Pallini R, Lotti F, Sette G *et al.* Chemotherapy resistance of glioblastoma stem cells. *Cell Death Differ* 2006; **13**: 1238–1241.
9. Hadjipanayis CG, Van Meir EG. Brain cancer propagating cells: biology, genetics and targeted therapies. *Trends Mol Med* 2009; **15**: 519–530.
10. Cheng CK, Fan QW, Weiss WA. PI3K signaling in glioma-animal models and therapeutic challenges. *Brain Pathol* 2009; **19**: 112–120.
11. De Witt, Hamer PC. Small molecule kinase inhibitors in glioblastoma: a systematic review of clinical studies. *Neuro Oncol* 2010; **12**: 304–316.
12. Ciceroni C, Arcella A, Mosillo P, Battaglia G, Mastrantoni E, Oliva MA *et al.* Type-3 metabotropic glutamate receptors negatively modulate bone morphogenetic protein receptor signaling and support the tumorigenic potential of glioma-initiating cells. *Neuropharmacology* 2008; **55**: 568–576.
13. Nicoletti F, Bockaert J, Collingridge GL, Conn PJ, Ferraguti F, Schoepp DD *et al.* Metabotropic glutamate receptors: from the workbench to the bedside. *Neuropharmacology* 2011; **60**: 1017–1041.
14. Stupp R, Gander M, Leyvraz S, Newlands E. Current and future developments in the use of temozolomide for the treatment of brain tumors. *Lancet Oncol* 2001; **2**: 552–560.
15. Fiory F, Oriente F, Miele C, Romano C, Trencia A, Alberobello AT *et al.* Protein kinase C-zeta and protein kinase B regulate distinct steps of insulin endocytosis and intracellular sorting. *J Biol Chem* 2004; **279**: 11137–11145.
16. Vivanco I, Sawyers CL. The phosphatidylinositol 3-kinase AKT pathway in human cancer. *Nat Rev Cancer* 2002; **2**: 489–501.
17. Weaver KD, Yeyeodu S, Cusack JC Jr, Baldwin AS Jr, Ewend MG. Potentiation of chemotherapeutic agents following antagonism of nuclear factor kappa B in human gliomas. *J Neuro Oncol* 2003; **61**: 187–196.
18. Shin HM, Kim MH, Kim BH, Jung SH, Kim YS, Park HJ *et al.* Inhibitory action of novel aromatic diamine compound on lipopolysaccharide-induced nuclear translocation of NF-kappaB without affecting IkappaB degradation. *FEBS Lett* 2004; **571**: 50–54.
19. Kopp E, Ghosh S. Inhibition of NF-kappa B by sodium salicylate and aspirin. *Science* 1994; **265**: 956–959.
20. Inoki K, Li Y, Zhu T, Wu J, Guan KL. TSC2 is phosphorylated and inhibited by Akt and suppresses mTOR signalling. *Nat Cell Biol* 2002; **4**: 648–657.
21. Argyriou AA, Kalofonos HP. Molecularly targeted therapies for malignant gliomas. *Mol Med* 2009; **15**: 115–122.
22. Gerson SL. MGMT: its role in cancer aetiology and cancer therapeutics. *Nat Rev Cancer* 2004; **4**: 296–307.
23. Bobustuc GC, Smith JS, Maddipatla S, Jeudy S, Limaye A, Isley B *et al.* MGMT inhibition restores ERα functional sensitivity to anti-estrogen therapy. *Mol Med* 2012; **18**: 913–929.
24. Kaina B, Margison GP, Christmann M. Targeting O^6-methylguanine-DNA methyltransferase with specific inhibitors as a strategy in cancer therapy. *Cell Mol Life Sci* 2010; **67**: 3663–3681.
25. Sontheimer H. Malignant gliomas: perverting glutamate and ion homeostasis for selective advantage. *Trends Neurosci* 2003; **26**: 543–549.
26. Lyons SA, Chung WJ, Weaver AK, Ogunrinu T, Sontheimer H. Autocrine glutamate signaling promotes glioma cell invasion. *Cancer Res* 2007; **67**: 9463–9471.
27. Buckingham SC, Campbell SL, Haas BR, Montana V, Robel S, Ogunrinu T *et al.* Glutamate release by primary brain tumors induces epileptic activity. *Nat Med* 2011; **17**: 1269–1274.
28. Yoshida Y, Tsuzuki K, Ishiuchi S, Ozawa S. Serum-dependence of AMPA receptor-mediated proliferation in glioma cells. *Pathol Int* 2006; **56**: 262–271.
29. Ishiuchi S, Yoshida Y, Sugawara K, Aihara M, Ohtani T, Watanabe T *et al.* Ca^{2+}-permeable AMPA receptors regulate growth of human glioblastoma via Akt activation. *J Neurosci* 2007; **27**: 7987–8001.
30. de Groot J, Sontheimer H. Glutamate and the biology of gliomas. *Glia* 2011; **59**: 1181–1189.
31. Schoepp DD, Jane DE, Monn JA. Pharmacological agents acting at subtypes of metabotropic glutamate receptors. *Neuropharmacology* 1999; **38**: 1431–1476.
32. Prasad G, Sottero T, Yang X, Mueller S, James CD, Weiss WA *et al.* Inhibition of PI3K/mTOR pathways in glioblastoma and implications for combination therapy with temozolomide. *Neuro Oncol* 2011; **13**: 384–392.
33. Lavon I, Fuchs D, Zrihan D, Efroni G, Zelikovitch B, Fellig Y *et al.* Novel mechanism whereby nuclear factor kappaB mediates DNA damage repair through regulation of O(6)-methylguanine-DNA-methyltransferase. *Cancer Res* 2007; **67**: 8952–8959.
34. Hegi ME, Diserens AC, Gorlia T, Hamou MF, de Tribolet N, Weller M *et al.* MGMT gene silencing and benefit from temozolomide in glioblastoma. *N Engl J Med* 2005; **352**: 997–1003.
35. Hegi ME, Liu L, Herman JG, Stupp R, Wick W, Weller M *et al.* Correlation of O^6-methylguanine methyltransferase (MGMT) promoter methylation with clinical outcomes in glioblastoma and clinical strategies to modulate MGMT activity. *J Clin Oncol* 2008; **26**: 4189–4199.
36. Eoli M, Menghi F, Bruzzone MG, De Simone T, Valletta L, Pollo B *et al.* Methylation of O^6-methylguanine DNA methyltransferase and loss of heterozygosity on 19q and/or 17p are overlapping features of secondary glioblastomas with prolonged survival. *Clin Cancer Res* 2007; **13**: 2606–2613.
37. Krex D, Klink B, Hartmann C, von Deimling A, Pietsch T, Simon M *et al.* Long-term survival with glioblastoma multiforme. *Brain* 2007; **130**: 2596–2606.
38. Martinez R, Schackert G, Yaya-Tur R, Rojas-Marcos I, Herman JG, Esteller M. Frequent hypermethylation of the DNA repair gene MGMT in long-term survivors of glioblastoma multiforme. *J Neurooncol* 2007; **83**: 91–93.
39. Park CK, Park SH, Lee SH, Kim CY, Kim DW, Paek SH *et al.* Methylation status of the MGMT gene promoter fails to predict the clinical outcome of glioblastoma patients treated with ACNU plus cisplatin. *Neuropathology* 2009; **29**: 443–449.
40. Minniti G, Salvati M, Arcella A, Buttarelli F, D'Elia A, Lanzetta G *et al.* Correlation between O^6-methylguanine-DNA methyltransferase and survival in elderly patients with glioblastoma treated with radiotherapy plus concomitant and adjuvant temozolomide. *J Neurooncol* 2010; **102**: 311–316.
41. Yang Y, Xia F, Hermance N, Mabb A, Simonson S, Morrissey S *et al.* A cytosolic ATM/NEMO/RIP1 complex recruits TAK1 to mediate the NF-kappaB and p38 mitogen-activated protein kinase (MAPK)/MAPK-activated protein 2 responses to DNA damage. *Mol Cell Biol* 2011; **31**: 2774–2786.
42. Piret B, Schoonbroodt S, Piette J. The ATM protein is required for sustained activation of NF-kappaB following DNA damage. *Oncogene* 1999; **18**: 2261–2271.
43. Volcic M, Karl S, Baumann B, Salles D, Daniel P, Fulda S *et al.* NF-κB regulates DNA double-strand break repair in conjunction with BRCA1-CtIP complexes. *Nucleic Acids Res* 2012; **40**: 181–195.
44. Miyamoto S. Nuclear initiated NF-κB signaling: NEMO and ATM take center stage. *Cell Res* 2011; **21**: 116–130.
45. Ricci-Vitiani L, Pedini F, Mollinari C, Condorelli G, Bonci D, Bez A *et al.* Absence of caspase 8 and high expression of PED protect primitive neural cells from cell death. *J Exp Med* 2004; **200**: 1257–1266.
46. Martini M, Pallini R, Luongo G, Cenci T, Lucantoni C, Larocca LM. Prognostic relevance of SOCS3 hypermethylation in patients with glioblastoma multiforme. *Int J Cancer* 2008; **123**: 2955–2960.

Supplementary Information accompanies the paper on Cell Death and Differentiation website (http://www.nature.com/cdd)